https://doi.org/10.5194/acp-2021-948
Preprint. Discussion started: 21 December 2021

Atmospheric Chemistry and Physics Discussions

Seasonal characteristics of atmospheric peroxyacetyl nitrate (PAN) in a coastal city of Southeast China: Explanatory factors and photochemical effects

Taotao Liu[1,2,3], Gaojie Chen[1,2,3], Jinsheng Chen[1,2]*, Lingling Xu[1,2], Mengren Li[1,2], Youwei Hong[1,2]*, Yanting Chen[1,2], Xiaoting Ji[1,2,3], Chen Yang[1,2,3], Yuping Chen[1,2,3], Weiguo Huang[4], Quanjia Huang[5], Hong Wang[6]

[1]Center for Excellence in Regional Atmospheric Environment, Institute of Urban Environment, Chinese Academy of Sciences, Xiamen, China
[2]Key Lab of Urban Environment and Health, Institute of Urban Environment, Chinese Academy of Sciences, Xiamen, China
[3]University of Chinese Academy of Sciences, Beijing, China
[4]State Key Laboratory of Structural Chemistry, Fujian Institute of Research on the Structure of Matter, Chinese Academy of Sciences, Fuzhou, China.
[5]Xiamen Environmental Monitoring Station, Xiamen, China
[6]Fujian Meteorological Science Institute, Fujian Key Laboratory of Severe Weather, Fuzhou, China

Corresponding authors E-mail: Jinsheng Chen (jschen@iue.ac.cn); Youwei Hong (ywhong@iue.ac.cn)

Abstract:

Peroxyacetyl nitrate (PAN) acting as a typical indicator of photochemical pollution can redistribute NOx and modulate O_3 production. Coupled with the observation-based model (OBM) and a generalized additive model (GAM), the intensive observation campaigns were conducted to reveal the pollution characteristics of PAN and its impact on O_3, the contributions of influencing factors to PAN formation were also quantified in this paper. The F-values of GAM results reflecting the importance of the influencing factors showed that ultraviolet radiation (UV, F-value=60.64), Ox (Ox=NO_2+O_3, 57.65), and air temperature (T, 17.55) were the main contributors in the PAN pollution in spring, while the significant effects of Ox (58.45), total VOCs (TVOCs, 21.63) and T (20.46) were found in autumn. The PAN formation rate in autumn was 1.58 times higher than that in spring, relating to the intense photochemical reaction and meteorological conditions. Without considering the transformation of peroxyacetyl radical (PA) and PAN, acetaldehyde contributed to the dominant production of PA (46±4%), followed by methylglyoxal (28±3%) and radical cycling (19±3%). The PAN formation was highly VOC-sensitive, and sufficient NOx (compared with VOCs abundance) would not be the limited factor for atmospheric photochemistry. PAN could promote or inhibit O_3 formation under high or low ROx levels, respectively. The PAN promoting O_3 formation mainly occurred during the periods of 11:00-16:00 (local time) when the favorable meteorological conditions (high UV and T) stimulated the photochemical reactions to offer ROx radicals, which accounted for 17% of the whole monitoring periods in spring and 31% in autumn. In this study, the formation mechanism of PAN and its effect on ozone were identified, which might be

https://doi.org/10.5194/acp-2021-948
Preprint. Discussion started: 21 December 2021


Atmospheric Chemistry and Physics Discussions

helpful to improve the scientific understanding of photochemical pollution in coastal areas.

Keywords: PAN formation mechanism; GAM model; OBM-MCM; Sensitivity analysis; Photochemical pollution; Coastal area

1 Introduction

Peroxyacetyl nitrate ($CH_3C(O)O_2NO_2$, PAN) is a key product of photochemical smog (Penkett and Brice, 1986; Li et al., 2019). PAN is generated through photochemical reactions of precursors emitted by human activities only, and the atmospheric PAN is a reliable and scientific indicator of photochemical pollution (Lonneman et al., 1976; Han et al., 2017). In the surface atmosphere, the level of PAN is much lower than that of ozone (O_3), but its biological toxicity is about one or two magnitudes greater than that of O_3 (Temple and Taylor, 1983). Additionally, PAN acts as a temporary reservoir for NOx and radicals, and can transport to remote regions to redistribute NOx and intervene in O_3 production at regional or even global scale (Kleindienst, 1994; Atkinson et al., 2006; Fischer et al., 2010).

The reaction of peroxyacetyl radical ($CH_3C(O)O_2$, PA) with NO_2 is solely formation pathway of PAN (Han et al., 2017; Xue et al., 2014). PAN affects radical chemistry and modulates O_3 production mainly by affecting PA radical, which is one of the most abundant organic peroxy radicals in the troposphere (Tyndall et al., 2001). Only a small group of oxygenated volatile organic compounds (OVOCs) (i.e. acetaldehyde (CH_3CHO), methacrolein (MACR), methyl vinyl ketone (MVK), methyl ethyl ketone (MEK), and methylglyoxal (MGLY)) can directly produce PA radical to generate PAN (Xue et al., 2014; Zhang et al., 2015). These OVOCs (the second-generation precursors of PAN) are mainly transformed by oxidation reactions from some hydrocarbons such as ethane, propene, isoprene and aromatics (the first-generation precursors of PAN) (Xu et al., 2021). The main and direct PAN destruction is thermal decomposition, and the indirect sinks of PAN were the reactions of PA with NO, HO_2, and RO_2 (Wolfe et al., 2014; Zeng et al., 2019).

Some studies on the distribution and sources of PAN have been conducted in urban, suburban, and remote regions around the world (Grosjean et al., 2002; Marley et al., 2007; Roberts et al., 2001). The mixing ratio of PAN in cities is higher than that in rural and remote areas, and that in background areas such as oceans and mountains can be as low as tens of pptv (Gaffney et al., 1999; Moore et al., 2009). Despite the growing concerns about photochemical pollution in China, PAN measurements and analysis of its photochemical mechanism are still sparse (Zeng et al., 2019). At present, the observations of PAN

https://doi.org/10.5194/acp-2021-948
Preprint. Discussion started: 21 December 2021

were mainly distributed in Beijing, Guangzhou, and Hong Kong (Xue et al., 2014; Yuan et al., 2018; Zeng et al., 2019). Xue et al. (2014) reported that anthropogenic VOCs were the most important precursors of PAN in urban areas, and isoprene was the predominant precursor in suburban regions. In Zeng et al. (2019) study, carbonyls offered the highest contribution to PAN production, followed by aromatics and BVOCs. In addition, some researchers found that atmospheric PAN suppressed local O_3 formation in autumn (Zeng et al., 2019). Recently, negative and positive impacts of PAN photochemistry on O_3 production were captured under the low and high NOx conditions, respectively. However, the PAN formation and its influencing mechanism on O_3 production are still complex and unclear (Hu et al., 2020; Zhang et al 2019; Xu et al., 2018). Long-term field measurements and model simulations could help to verify the mechanisms under various pollution scenarios and environmental conditions.

Xiamen, with meteorological conditions of strong radiation, high relative humidity and air temperature, is located in the coastal region of Southeast China (Liu et al., 2020a; Liu et al., 2020b). Rapid urbanization has caused photochemical pollution in the coastal city, with relatively high levels of nitrogen oxides and volatile organic compounds. Our previous studies focused on the occurrence and pollution characteristics of PAN (Hu et al., 2020). In this study, an observation-based model coupled to the Master Chemical Mechanism (OBM-MCM) was used to better understand PAN photochemistry, and a generalized additive model (GAM) was adopted to quantify the complex nonlinear relationships of PAN with its precursors and environmental factors (Hua et al., 2021). The study aims to explore (1) the PAN formation mechanism and sensitivity analysis, (2) the impacts of PAN on O_3 formation and radical chemistry, (3) the relationship between PAN and influencing factors under different pollution scenarios.

2 Materials and methods

2.1 Study site and observations

https://doi.org/10.5194/acp-2021-948
Preprint. Discussion started: 21 December 2021

Atmospheric Chemistry and Physics Discussions

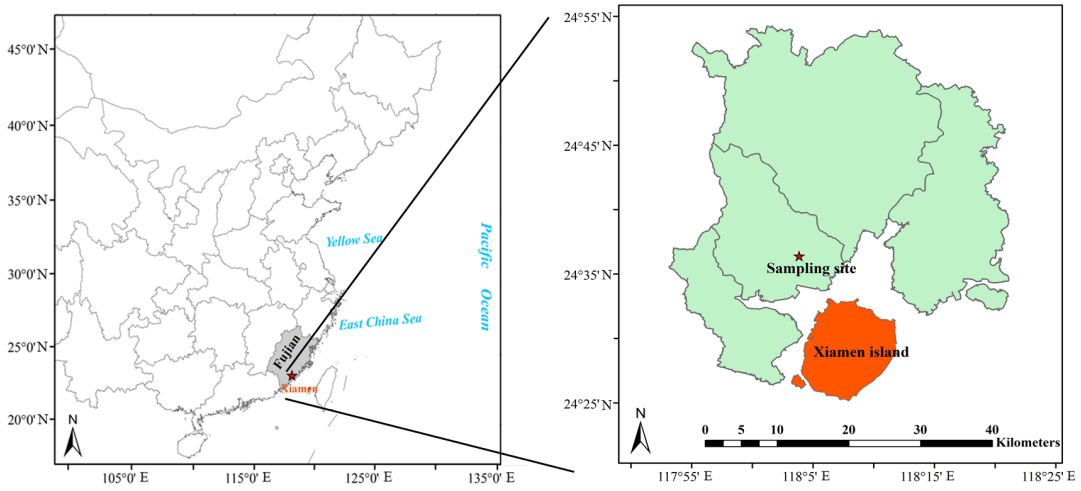

Fig. 1. Location of Xiamen and the observation site.

Observations were carried out at the Atmospheric Environment Observation Supersite (AEOS, 24.61° N, 118.06° E; Fig. 1), located on the rooftop of around a 70 m high building in the Institute of Urban Environment, Chinese Academy of Sciences. The observations site is surrounded by highways, educational institutions, and residential buildings, which was characterized by rapidly urbanizing development area. When the prevailing wind direction was southerly winds, our observation site was attributed to the downwind region of the downtown (Xiamen island) with densely population and heavy traffic (Hu et al., 2020; Liu et al., 2021a). The field observation was continuously conducted from March 15 to November 4, 2020. The photochemical pollution events mainly appeared during spring and autumn in Xiamen, and we preferred to choose the periods with relatively high O_3 and PAN levels, then the measured data of 53 days in each season was chosen after excluding some special circumstances, such as extreme synoptic situations and instrument calibration. Xiamen is under the East Asian monsoon control, belonging to the subtropical marine climate. In spring, north cold airflow and south warm airflow formed the quasistationary front causing atmospheric stagnation. In autumn, under the control of the west pacific subtropical high (WPSH), high T and low RH enhanced the formation and accumulation of photochemical pollutants (Wu et al., 2020).

PAN was monitored using a PAN analyzer (PANs-1000, Focused Photonics Inc., Hangzhou, CN) containing gas chromatography with electron capture detector (GC-ECD). During the observation period, multi-point standard curve calibration was conducted once a month, and single-point calibration was conducted every week, respectively. In the calibration mode of the PAN analyzer, the Mass Flow Controller (MFC) controls the flow rate of NO, acetone and zero gas separately. The PAN standard gas is

https://doi.org/10.5194/acp-2021-948
Preprint. Discussion started: 21 December 2021


Atmospheric Chemistry and Physics Discussions

generated by the reaction of NO and acetone under ultraviolet light irradiation, and the sample is diluted to the required calibration mixing ratio for injection analysis. PAN was detected every 5 min and the detection limit was 50 pptv. The uncertainty and precision of PAN measurement were ±10% and 3%, respectively. Criteria air pollutants of O_3, CO, SO_2, and NOx, were monitored by using Thermo Instruments TEI 49i, 48i, 43i, and 42i (Thermo Fisher Scientific, Waltham, MA, USA), respectively. Particulate matters ($PM_{2.5}$) were monitored by oscillating microbalance with tapered element (TEOM1405, Thermo Scientific Corp., MA, US), and the uncertainty of the $PM_{2.5}$ measurement was ±20%, respectively. The meteorological parameters (i.e. wind speed (WS), wind direction (WD), pressure (P), air temperature (T), and relative humidity (RH)) were measured by an ultrasonic atmospherium (150WX, Airmar, USA). Ultraviolet radiation (UV) was determined by a UV radiometer (KIPP & ZONEN, SUV5 Smart UV Radiometer). HONO was monitored using an analyzer for Monitoring Aerosols and Gases in Ambient Air (MARGA, ADI 2080, Applikon Analytical B.V., the Netherlands). A gas chromatography-mass spectrometer (GC-FID/MS, TH-300B, Wuhan, CN) was used for monitoring the atmospheric VOCs with a 1-hour time resolution. The single-point calibration was performed every day at 23:00 with the standard mixtures of PAMS and TO15, and multi-point calibration was performed one month. The detection limits of the measured VOCs were in the range of 0.02 ppbv to 0.30 ppbv, and the measurement precision was $\leqslant$10%. Photolysis frequencies including $J(O^1D)$, $J(NO_2)$, J(HONO), $J(NO_3)$, J(HCHO), and $J(H_2O_2)$ were analyzed by a photolysis spectrometer (PFS-100, Focused Photonics Inc., Hangzhou, China), and the uncertainty and detection limit of photolysis rates measurement were ±5% and around 1×10^{-5}, respectively. Table S1 shows the detailed uncertainty and detection limit of instruments for trace gas observation. A schedule was applied to operate and inspect the AEOS monitoring station regularly and strictly to ensure the validity of the data. The detailed applications of the atmospheric monitoring procedure were shown in our previous studies (Wu et al., 2020; Liu et al., 2020a; Liu et al., 2020b; Hu et al., 2020).

2.2 Observation-based model

The OBM-MCM model is successfully used in the simulation of photochemical processes and the quantification of the reaction rates, such as O_3, PAN and alkyl nitrates ($RONO_2$) (Zeng et al. 2019). In our study, the PAN photochemistry mechanism was simulated using this box model, and the incorporated chemical mechanism was the latest version of MCM-v3.3.1 (http://mcm.leeds.ac.uk/MCM/), which introduced 142 nonmethane VOCs and about 20000 elementary reactions (Jenkin et al., 2003; Saunders

https://doi.org/10.5194/acp-2021-948
Preprint. Discussion started: 21 December 2021


Atmospheric Chemistry and Physics Discussions

et al., 2003). The physical process including dilution effect and dry deposition within the boundary layer height was considered, avoiding the excessive accumulation of pollutants in the model (Li et al., 2018; Liu et al., 2021; Xue et al., 2016). The observed data with a time resolution of 1 h of pollutants, meteorological parameters, and photolysis rate constants, which were mentioned in Section 2.1, were input into the OBM-MCM model as constraints. The photolysis rates of other molecules were driven by solar zenith angle and were scaled by measured JNO_2 (Saunders et al., 2003). Pre-ran for 2 days before running the model to constrain the unmeasured compounds reaching a steady-state (Xue et al., 2014). The detailed model introduction showed in our previous study (Liu et al., 2021a).

PAN affects atmospheric photochemistry by acting as a temporary source or sinks of PA radical (Xue et al., 2014; Liu et al., 2021), hence the production and sink of PA radical reflecting the PAN formation were discussed in our study. Furthermore, relative incremental reactivity (RIR) was used to analyze the sensitivity of O_3 (Eq. 1) and PAN (Eq. 2) to their precursors, and was calculated as the ratio of the differences in O_3 or PAN net production rate to variety in precursors (Chen et al., 2020; Liu et al., 2021). The detailed net production rate of O_3 ($P(O_3)$) was introduced in our previous study (Liu et al., 2021a). The net production of PAN (P(PAN)) involved the production pathway of $PA+NO_2$, and the loss of PAN was thermal decomposition and PAN+OH (Zeng et al., 2019).

$$RIR(PAN) = \frac{\Delta P(O_3)/P(O_3)}{\Delta X/X} \quad (1)$$

$$RIR(O_3) = \frac{\Delta P(PAN)/P(PAN)}{\Delta X/X} \quad (2)$$

Here, the $\Delta X/X$ meaning the reduction in the input mixing ratios of each target O_3 and PAN precursor group was 20% (Liu et al., 2021).

2.3 Generalized additive model

The Generalized Additive Model (GAM) is an extension of the additive model proposed. Different from traditional regression models, GAM is a non-parametric regression model driven by data rather than statistical distribution models (He et al., 2017). GAM does not need to set the parameter model in advance, and it can adjust the functional form of the explained variable according to the specific situation. The Generalized Additive Model (GAM) has been widely used in air pollution research such as O_3 and $PM_{2.5}$, and can effectively deal with the complex nonlinear relationship between air pollutants and influencing factors (Ma et al., 2020; Hua et al., 2021; Guan et al., 2019). It is the first time that the GAM is used to analyze the relationship between PAN and its influencing factors, and the combined effect of multiple influencing factors on the PAN mixing ratio was discussed in our study. Its form is:

https://doi.org/10.5194/acp-2021-948
Preprint. Discussion started: 21 December 2021

Atmospheric Chemistry and Physics Discussions

$$g(y)=\beta+f_1(x_1)+f_2(x_2)+\ldots\ldots+f_n(x_n)+\alpha \quad (3)$$

Where y is the response variable; $g(y)$ is the connection function; x_n, x_i, x_j, x_k, and x_l are the explanatory variables; fn is the non-parametric smoothing functions; β is the intercept; α is the truncation error.

The F-value, P-value, adjust R^2, and deviance explained given by the GAMs model are used to judge the significance of the influencing factors on PAN and the goodness of the model simulation. Among them, a high F-value indicates the great importance of the influencing factor; the P-value is used to judge the significance of the model result; the adjusted R^2 is the value of the regression square ranging from 0 to 1; the deviance explained represents the fitting effect. In addition, when the degree of freedom (edf, ref.df) of the explanatory variable is 1, it indicates that the explanatory variable and the response variable are linear. When the degree>1, it is a non-linear relationship.

3 Results and discussion

3.1. Overview of observation

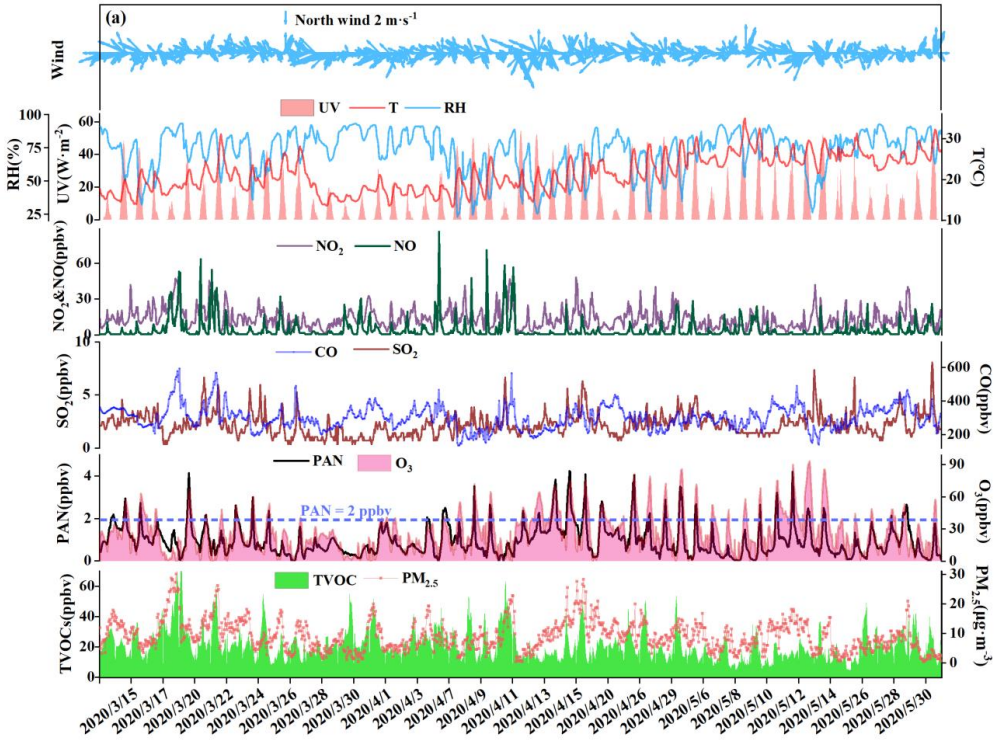

https://doi.org/10.5194/acp-2021-948
Preprint. Discussion started: 21 December 2021

Atmospheric Chemistry and Physics Discussions

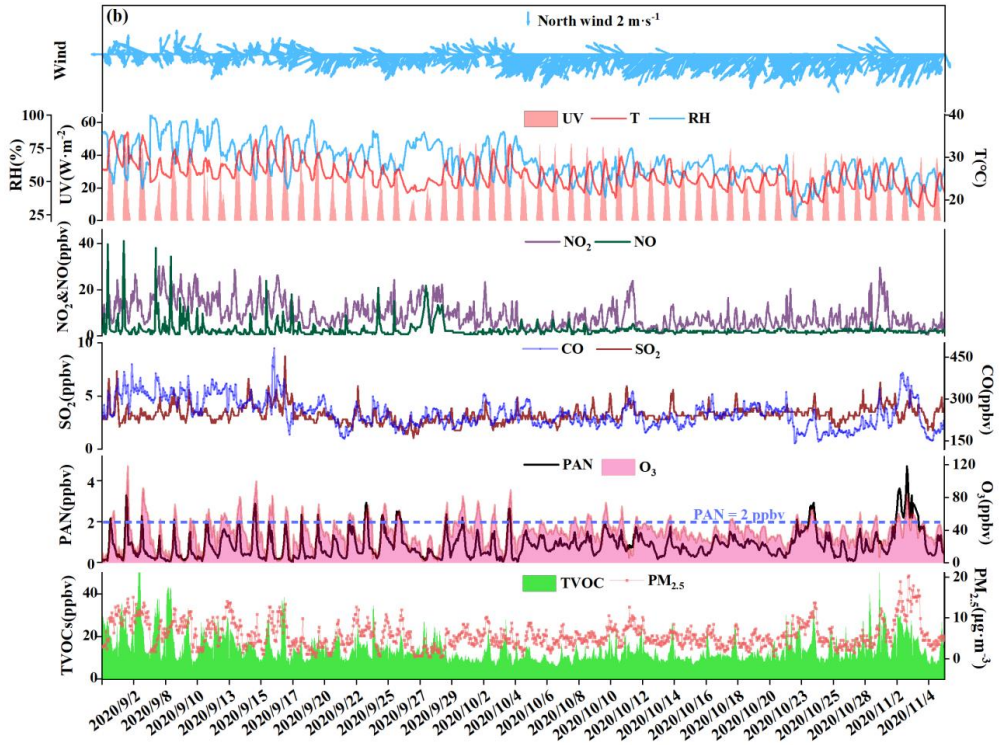

Fig. 2. Time series of PAN, O_3, NOx, CO, SO_2, TVOCs, $PM_{2.5}$, and meteorological parameters in (a) spring and (b) autumn.

The time series of air pollutants and meteorological parameters are shown in Fig. 2. The average levels of PAN in autumn (0.87±0.66 ppbv) were comparable to that in spring (0.96±0.73 ppbv), while O_3 mixing ratios in autumn (37.22±16.89 ppbv) were 1.39 times higher than that in spring (26.73±18.63 ppbv). PAN and O_3 are produced by the photochemical reactions of VOCs and NOx, thus they usually show a relatively close relationship ($R^2 \geq 0.49$, Fig. S1). The PAN level (0.92±0.69 ppbv) in Xiamen was lower than that of megacities such as Beijing (3.79±3.26 ppbv) (Xu et al., 2021), Jinan (2.54 ppbv) (Liu et al. 2018), Santiago (6.4 ppbv) (Rubio et al., 2005) and Chongqing (2.05 ppbv) (Sun et al., 2020), and was comparable to the coastal cities with relatively clean air, including Shenzhen (1.01±0.94 ppbv) (Xia et al., 2021), and Qingdao (0.81 ppbv) (Liu et al., 2021).

The averaged values of PAN and NO, NO_2, CO, TVOCs in spring were 1.70, 1.32, 1.21, and 1.46 times higher than those in autumn, respectively. The details of measured VOCs were provided in Table S2. Alkanes, OVOCs, aromatics and halocarbons accounted for about 90% of total VOCs, suggesting the impacts of atmospheric oxidation capacity and marine emissions in coastal regions (Liu et al., 2020a; Liu

https://doi.org/10.5194/acp-2021-948
Preprint. Discussion started: 21 December 2021

Atmospheric Chemistry and Physics Discussions

et al., 2020b). The wind directions in late spring and early autumn were messy due to the season switch. The wind rose charts showed that the wind direction frequencies with relatively high wind speed in spring and autumn were southeast wind and northeast wind (Fig. S2). Although the frequency of northwest wind (NNW) also accounted for a certain proportion, the NNW speeds were generally slow, and the direction of the NNW was mainly rural residential and mountainous areas with less anthropogenic emissions, so that it was not the focus of this research. The ultraviolet radiation (UV), WS and T in spring (15.32 $W \cdot m^{-2}$; 1.96 $m \cdot s^{-1}$; 21.51 ℃) were weaker than those in autumn (18.43 $W \cdot m^{-2}$; 3.01 $m \cdot s^{-1}$; 25.85 ℃), and RH and P in spring (73.25 %; 1010.71 hPa) were higher than that in autumn (65.21 %; 1008.71 hPa). These meteorological conditions carried by the WPSH (high T, low RH, and stagnant weather conditions) were conducive to the photochemical reaction and accumulation of air pollutants in autumn (Wu et al., 2019; Xia et al., 2021). High mixing ratios of PAN precursors in spring were conducive to the continuous and stable production of PAN, and the high air temperature in autumn accelerated the thermal decomposition of PAN. However, the O_3 levels in autumn were higher than that in spring, attributing to the influence of strong photochemical reaction conditions, regional transport from the Yangtze River Delta region or increased atmospheric background levels (Monks, 2000). High O_3 values in both seasons were concentrated on the wind direction of southeast and northeast (Fig. S3). We calculated the PAN lifetime in our previous study (Hu et al., 2020). The PAN lifetimes were 6.39 and 2.02 hours in spring and autumn, respectively. High PAN values easily happened in the wind direction of the southeast with low wind speed (<3 $m \cdot s^{-1}$) in spring, and northeast with a relatively high wind speed (from Quanzhou city, an industrial city adjacent to Xiamen) in autumn. Accordingly, O_3 showed obvious characteristics of long-range transport, and PAN pollution was mainly from local production/accumulation.

Based on the above analysis, we found that the photochemical reactions were still intense and even stronger under the condition of low precursor mixing ratios. Although the precursor mixing ratios of PAN and O_3 in spring were significantly higher than those in autumn ($P<0.01$), the PAN mixing ratios were comparable to and O_3 mixing ratios were much higher in autumn than those in spring, respectively. Therefore, it is very necessary to furtherly explore the key influencing factors and their formation mechanisms.

3.2 The influencing factors of PAN using the GAM

PAN levels are not only related to chemical reactions in the boundary layer, but also affected by meteorological conditions (Hu et al., 2020). According to the collinearity analysis (He and Lin, 2017), the

https://doi.org/10.5194/acp-2021-948
Preprint. Discussion started: 21 December 2021

Atmospheric Chemistry and Physics Discussions

meteorological parameters (UV, T, RH and WS) and other air pollutants (NO, TVOCs, $PM_{2.5}$ and O_x) were considered into the multiple-factor GAM model (Table S3). As shown in Table 1, the adjusted R^2 and deviance explained for the smoothed variables of the multiple-factor GAM model were 0.70 and 72% in spring, 0.60 and 63% in autumn. According to the F-values, the orders of the explanatory variables in spring and autumn were UV (60.64) > Ox (57.65) > T (17.55) > $PM_{2.5}$ (9.94) > TVOCs (9.52) > NO (8.73)> WS (7.42) > RH (3.4) and Ox (58.45) > TVOCs (21.63) > T (20.46) > $PM_{2.5}$ (14.53) > RH (10.99) > UV (7.13) > NO (4.16) >WS (2.55), respectively.

Response curves of the PAN mixing ratio to explanatory factors in the multiple-factor model were presented (Fig. 3 and Fig. S4). In spring, except for UV and T, the degrees of freedom (df) of the explanatory variables were greater than 1, indicating the non-linear relationships between explanatory variables and PAN. The PAN in both seasons showed a downward trend with the increase of NO, while the PAN in spring was unchanged with the fluctuation of NO. As we all know, the reaction of PA+NO is one of the most important loss pathways of PA, suggesting the fact that NO consumed PAN indirectly (Liu et al., 2021). Ox had a positive correlation with PAN, representing the promotion effects of atmospheric oxidation capacity on PAN formation. With the increase of TVOCs and $PM_{2.5}$ levels, PAN showed an upward trend. UV also had a significant positive correlation with PAN. However, the air temperature had a significant negative correlation with PAN, due to the thermal decomposition of PAN. In addition, when RH was more than 40%, the increase of RH was unfavorable for PAN production in both seasons. Some studies also found that high water vapor content could remove PAN and its precursors, thus reducing solar ultraviolet radiation to affect the photochemical reaction of PAN (Yan et al., 2018; Ma et al., 2020). Simultaneously, RH could affect the heterogeneous reactions by influencing viscosity and the phase diffusion of aerosol particulates (Li et al., 2013; Slade et al., 2014). Overall, the major factors of PAN formation in spring were UV, Ox, and T, while those factors including Ox, TVOCs, T and $PM_{2.5}$ played important roles in autumn.

Table 1 Estimated degree of freedom (Edf), degree of reference freedom (Ref. df), P-value, F-value, deviance explained (%), adjusted R^2, deviance contribution (%) for the smoothed variables in the multiple-factor GAM model.

Smoothed variables	Spring				Autumn			
	Edf	Ref.df	F-value	P-value	Edf	Ref.df	F-value	P-value
NO (ppbv)	5.21	6.26	8.73	0.00	1.11	1.21	4.16	0.03
Ox (ppbv)	4.73	5.85	57.65	0.00	4.84	5.98	58.45	0.00
TVOCs (ppbv)	7.14	8.19	9.52	0.00	4.08	5.06	21.63	0.00
$PM_{2.5}$ (ppbv)	5.73	6.86	9.94	0.00	1.53	1.90	14.53	0.00
UV ($W \cdot m^{-2}$)	1.00	1.00	60.64	0.00	4.38	5.38	7.13	0.00

https://doi.org/10.5194/acp-2021-948
Preprint. Discussion started: 21 December 2021

Atmospheric Chemistry and Physics Discussions

T (℃)	1.00	1.00	17.55	0.00	2.73	3.46	20.46	0.00
RH (%)	6.78	7.87	3.40	0.00	6.56	7.68	10.99	0.00
WS ($m \cdot s^{-1}$)	5.22	6.37	7.42	0.00	5.12	6.28	2.55	0.02
	Deviance explained (%)=80%; Adjust R^2=0.79				Deviance explained (%)=72%; Adjust R^2=0.70			

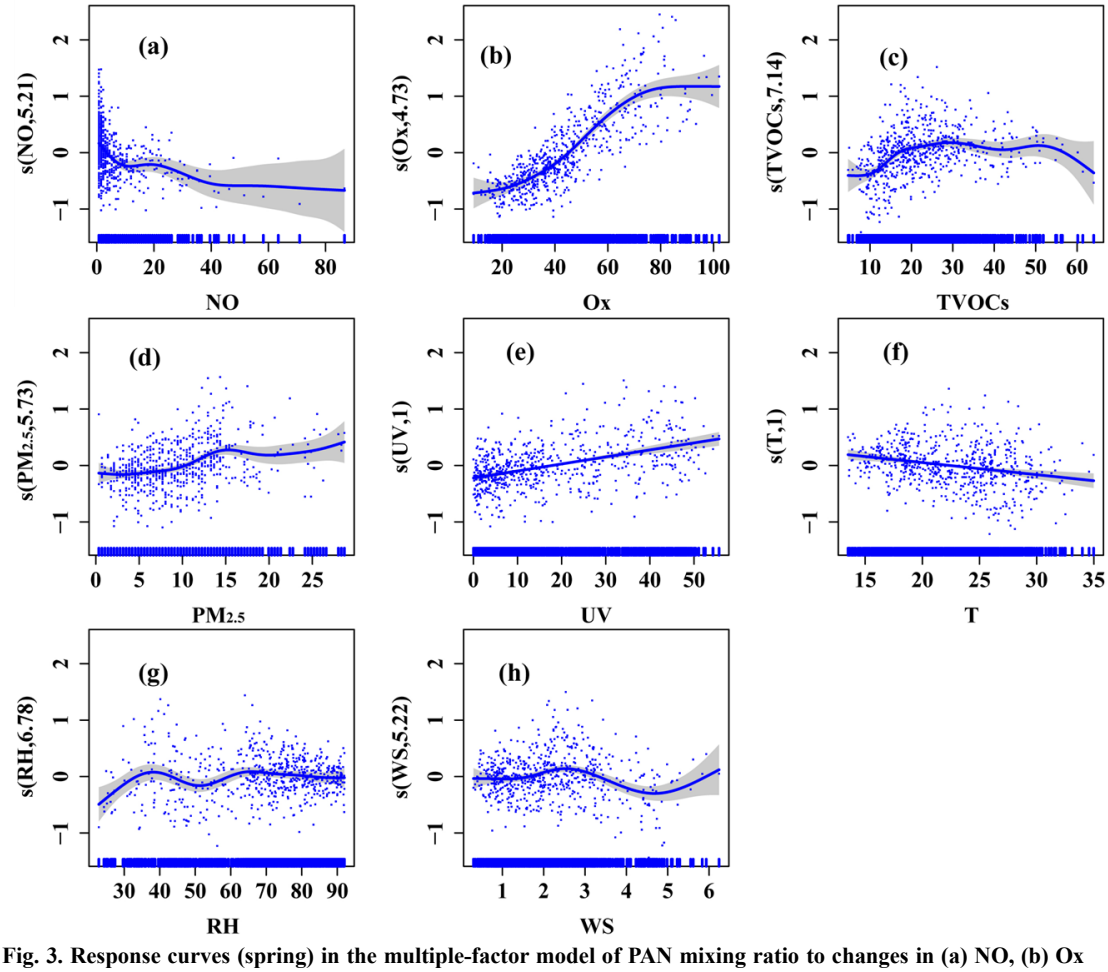

Fig. 3. Response curves (spring) in the multiple-factor model of PAN mixing ratio to changes in (a) NO, (b) Ox (Ox=O_3+NO_2), (c) TVOCs, (d) $PM_{2.5}$, (e) ultraviolet radiation (UV), (f) air temperature (T), (g) relative humidity (RH), and (h) wind speed (WS). The y-axis is the smoothing function values. For example, s(NO, df) shows the trend in PAN when NO changes, and the number of df is the degree of freedom. The x-axis is the influencing factor, and the shaded area around the solid red line indicates the 95% confidence interval of PAN. The blue vertical short lines represent the concentration distribution characteristics of the explanatory variables (units: NO (ppbv), Ox (O_3+NO_2) (ppbv), TVOCs (ppbv), $PM_{2.5}$ (ppbv), UV ($W \cdot m^{-2}$), T (℃), RH (%), WS ($m \cdot s^{-1}$)).

3.3. Formation mechanism of PAN

3.3.1 Diurnal variation during episodes and non-episodes

https://doi.org/10.5194/acp-2021-948
Preprint. Discussion started: 21 December 2021

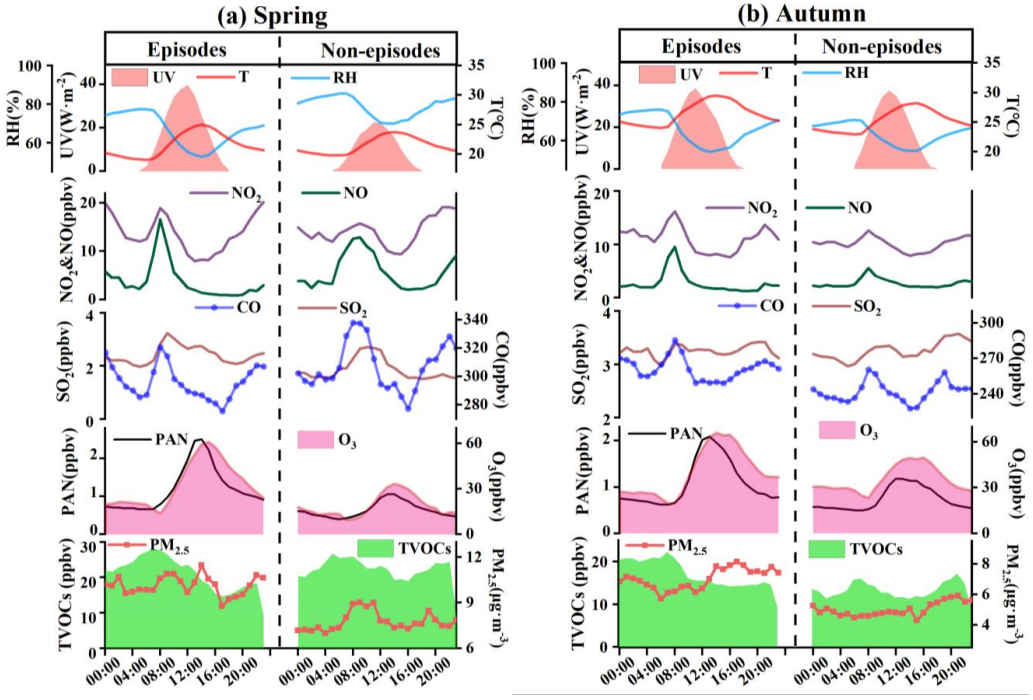

Fig. 4. Diurnal trends of PAN, O_3, TVOCs, $PM_{2.5}$, other trace gases and meteorological parameters during episodes and non-episodes in (a) spring and (b) autumn, respectively.

Throughout the 53-days campaign, 30 and 21 days (i.e., 57% and 40%) with the peak values of PAN exceeding 2 ppbv were observed in spring and autumn, respectively. The scenarios of episodes and non-episodes were classified, according to the previous method (Xue et al., 2014). Diurnal variations of air pollutants and meteorological parameters during episodes and non-episodes are shown in Fig. 4. PAN reached a maximum value at 14:00 (episodes) and 13:00 (non-episodes) in spring, while 13:00 (episodes) and 12:00 (non-episodes) were observed in autumn, related to UV radiation intensity. Compared with PAN, the O_3 peak was delayed by 1-2 hours, due to the accelerated decomposition of PAN at high air temperatures. The lowest PAN and O_3 mixing ratios in the early morning were caused by the all-night thermal decomposition without the photochemical formation and the NO titration during rush hour traffic, respectively (Zhang et al., 2015a; Elshorbany et al., 2008). A relatively broad peak of PAN and O_3 in autumn reflected the influence of regional transport (Zeng et al., 2019). Due to the photochemical reactions, the precursors of CO, NOx and VOCs were consumed during the daytime, and were accumulated during the nighttime with weak solar radiation. CO, NOx and TVOCs showed the highest levels at around 08:00 LT due to the nighttime accumulation and vehicle exhaust, but showed relatively low levels during the daytime, emphasizing the importance of frequent human activities and weather

https://doi.org/10.5194/acp-2021-948
Preprint. Discussion started: 21 December 2021

Atmospheric Chemistry and Physics Discussions

conditions. PAN and O_3 are secondary pollutants depending on both the levels of precursors and photochemical reactions. Therefore, the trends of PAN and O_3 were opposite to that of their precursors.

In autumn, averaged PAN and O_3 during episodes (PAN: 1.08±0.87 ppbv, and O_3: 40.06±20.27 ppbv) were higher than those during non-episodes (PAN: 0.74± 0.41 ppbv, and O_3: 35.36±13.95 ppbv). Meanwhile, some air pollutants and meteorological parameters during episodes were 1.03-1.40 times higher than those during non-episodes. The rainfall in Xiamen is more frequent in spring (Hu et al., 2020), leading to the obvious differences in UV and RH levels between episodes and non-episodes. In spring, the precursors (CO, NOx, TVOCs) of PAN during episodes were 1.04-1.49 times lower than those during non-episodes. Moreover, the PAN and O_3 mixing ratios during episodes (PAN: 1.20±0.81 ppbv, and O_3: 32.92±19.81 ppbv) were still significantly higher than those during non-episodes (PAN: 0.64±0.43 ppbv, and O_3: 18.65±13.16 ppbv), attributing to the favorable meteorological conditions of photochemical reactions (strong UV, high T and low RH). These results further explained that UV, Ox, and T in spring and Ox, TVOCs, T and $PM_{2.5}$ in autumn played important roles in the formation of PAN based on the GAM analysis.

3.3.2. Formation and loss of PA radical

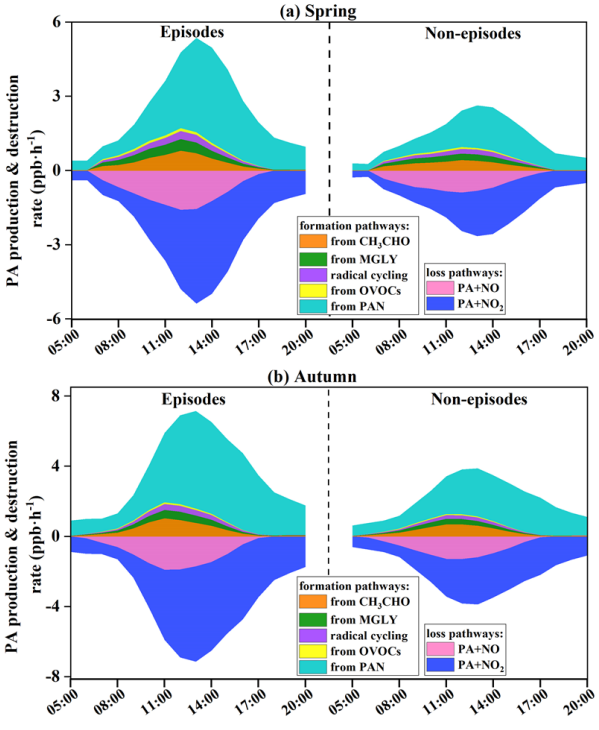

Fig. 5. Formation and destruction rates of PA radical (hence PAN) during episodes and non-episodes in (a) spring

https://doi.org/10.5194/acp-2021-948
Preprint. Discussion started: 21 December 2021


Atmospheric Chemistry and Physics Discussions

and (b) autumn, respectively.

The formation and sink pathways of PA radical were further explored under different pollution scenarios (Fig. 5). Both the PA (hence PAN) production and destruction rates during episodes were 1.80 times higher than those during non-episodes. Combined with the analysis of Section 3.3.1, PA production rates during the daytime (06:00-17:00 LT) in autumn were 1.58 times higher than that in spring, even though the precursor levels in autumn were much low compared to those in spring. These results indicated favorable meteorological conditions producing and accumulating pollutants and local transport bringing high air pollutants from Quanzhou city or urban plumes were dominant factors for the strong PAN production rates. The thermal decomposition of PAN to PA radical in autumn accounted for 77±12% (episodes) and 73±16% (non-episodes) of total PA production, as well as 70±12% (episodes) and 64±15% (non-episodes) in spring, attributing to the relatively high air temperature and UV intensity. The thermal decomposition of PAN peaked at around 13:00~14:00 LT, when the air temperature was the highest in the day, and the pathways without considering the transform between PA and PAN peaked at noontime around 12:00 LT, when the solar radiation was the highest and photochemical reactions became the most intensive.

The average daytime PAN production rate from CH_3CHO by reacting with OH and NO_3 contributed 0.36±0.25 ppb h^{-1} and 0.24±0.13 ppb h^{-1} during episodes and non-episodes in spring. While the rate of 0.46±0.35 ppb h^{-1} and 0.34±0.24 ppb h^{-1} during episodes and non-episodes were observed in autumn. The second production reaction was photolysis and oxidation by OH and NO_3 of MGLY (episode: 0.25±0.15 ppb h^{-1} and non-episodes: 0.17±0.08 ppb h^{-1} in spring; episode: 0.24±0.17 ppb h^{-1} and non-episodes: 0.16±0.11 ppb h^{-1} in autumn). Then, the processes of radical cycling including RO radical decomposition and reactions of acyl peroxy radicals with NO were also the important sources to produce PA, with the contributions of 20±3% and 18±3% in spring and autumn. PA from the other OVOCs (not including CH_3CHO, MGLY, MVK, MACR and acetone) through reactions of photolysis and oxidation by OH, NO_3, and O_3, accounted for 7±2% and 6±1% in spring and autumn, respectively. Other reactions of acetone, MVK, MACR, MPAN and isoprene had a minor contribution (around 1% in total) to PA formation. In contrast, the major contributor of PAN destruction rate was PA+NO_2 (69±16% in spring and 73±14% in autumn), followed by PA+NO (31±17% and 27±13%), while the other reactions with NO_3, HO_2 and RO_2 contributed limitedly (around 0.1% of the total).

3.3.3. Sensitivity of PAN precursors

https://doi.org/10.5194/acp-2021-948
Preprint. Discussion started: 21 December 2021

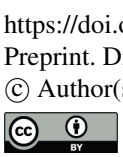

Atmospheric Chemistry and Physics Discussions

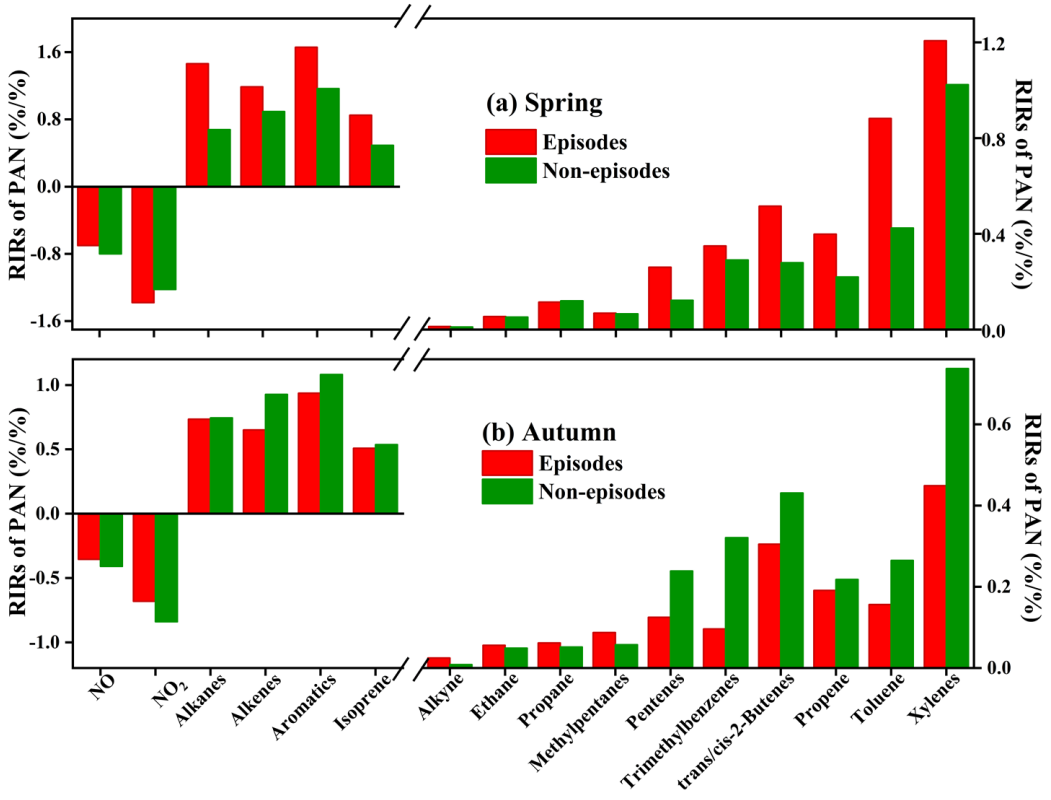

Fig. 6. The OBM-MCM calculated relative incremental reactivity (RIR) for major PAN precursor groups and specific species in (a) spring and (b) autumn during the daytime (06:00-17:00 LT).

The OBM-MCM model analysis could be used to examine the relationship between PAN and its precursors, and quantify the contribution of first-generation precursors (Liu et al., 2021; Cardelino and Chameides, 1995). The relative incremental reactivities (RIRs) for O_3 and PAN are shown in Fig. 6 and Fig. S5. The PAN production was highly VOCs-sensitive, while the RIRs of NO and NO_2 were negative ranging from –0.17 to –1.94%/% during the daytime (06:00-17:00 LT). This consisted of the fact that high dense mobiles resulted in the large emissions of vehicle exhausts in Xiamen city. The ratio of VOCs/NOx (1.11±0.32) also convinced NOx was not the limited factor on the photochemical reaction (Tan et al., 2019). In suburban or rural areas, the transition regime and NOx-sensitive for PAN and O_3 production were usually found (Xue et al., 2014; Liu et al., 2021). Zeng et al. (2019) found NO_2-positive and NO-negative to PAN formation in a suburban of Hong Kong, consisting with the fact that NO_2 directly produced PAN and NO consumed PA radical inhibiting PAN formation.

As shown in Fig.6, aromatics showed the largest RIRs for PAN in spring (1.41%/%) and autumn (1.03%/%), followed by alkanes (1.04%/% in spring and 0.78%/% in autumn), Alkenes (1.04%/% and

https://doi.org/10.5194/acp-2021-948
Preprint. Discussion started: 21 December 2021


Atmospheric Chemistry and Physics Discussions

368 0.74%/%), and isoprene (0.67%/% and 0.52%/%). The sensitivities of PAN precursors in spring were
369 1.37-2.07 times higher than those in autumn, due to the large percentages of PAN decomposition at high
370 air temperatures in autumn. In spring, the weak solar radiation led to poor photochemical reactions, so
371 the RIRs of PAN during non-episodes were lower than that during episodes. However, the PAN
372 sensitivities during episodes were lower than those during non-episodes, attributed to the rapid PAN
373 decomposition in autumn (Liu et al., 2021). In addition, RIRs of VOCs and NOx for PAN were
374 significantly higher than that of O_3 (Fig. S5). For RIRs of VOCs, except for air temperature, the different
375 formation mechanisms of PAN and O_3 should be considered. Only a small part of the VOCs could produce
376 PA to form PAN, thereby, the VOCs were insufficient to produce PAN (Fischer et al., 2014). For RIRs of
377 NOx, O_3 was produced from the NO_2 conversion process, and was also rapidly consumed by NO titration.
378 High mixing ratios of VOCs and NOx enhanced the PAN formation, even though a pathway of NO
379 destructed PAN, which was negligible compared to thermal decomposition. For this reason, the RIRs of
380 NOx for PAN were higher than those for O_3.

381 In addition, the key first-generation VOCs species (including xylenes, toluene trans/cis-2-butenes,
382 trimethylbenzenes, propene, pentenes, and methypentanes) governing PAN production were further
383 identified (Fig. 6). The results suggested that the reduction of aromatics, alkenes and alkanes with ≤5
384 carbons could effectively decrease PAN pollution.

385

386 **3.4. Impacts of PAN on O_3 formation**

https://doi.org/10.5194/acp-2021-948
Preprint. Discussion started: 21 December 2021

Atmospheric Chemistry and Physics Discussions

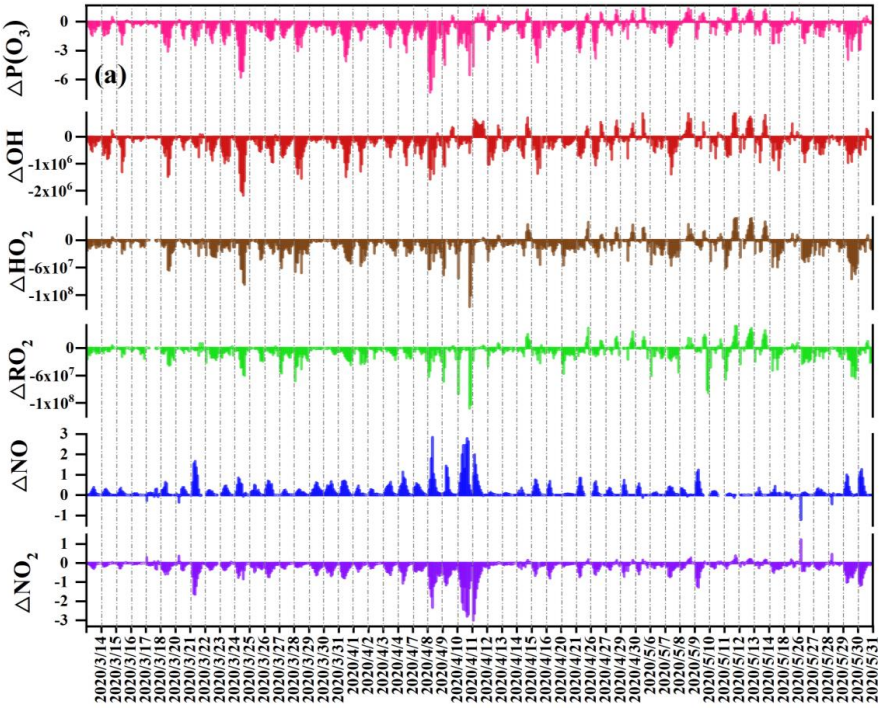

387

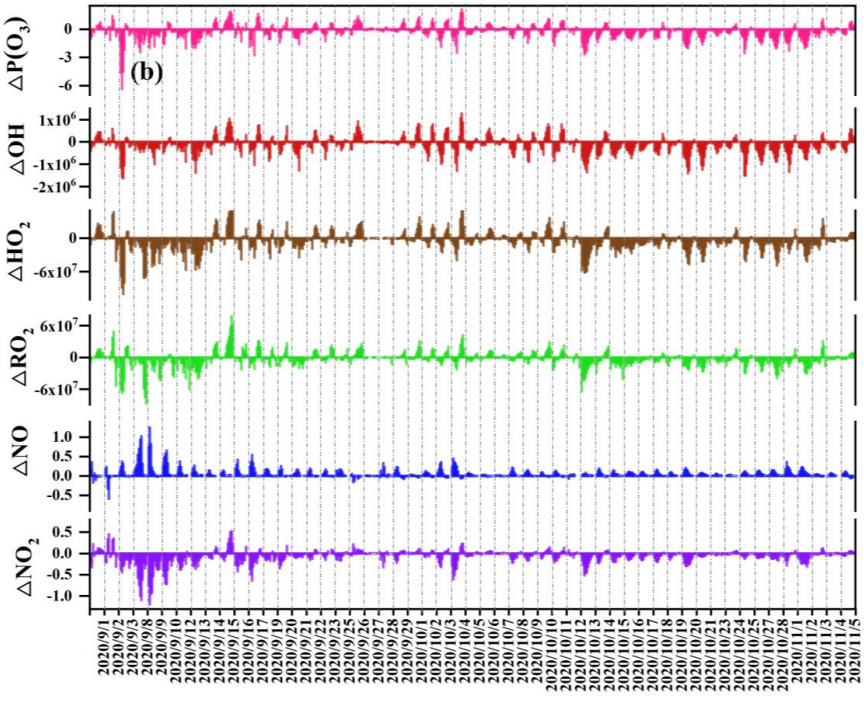

388

389 **Fig. 7. The differences of O_3 net production △P(O_3), △OH, △HO_2, △RO_2, △NO and △NO_2 between the SC1**
390 **and the SC2 during the daytime (06:00-17:00) in (a) spring and (b) autumn (Unit: ppbv·h^{-1} for △P(O_3); ppbv for**
391 **△NO and △NO_2; molecules·cm^{-3} for △OH, △HO_2 and △RO_2). The SC1 scenario was the base scenario putting**

https://doi.org/10.5194/acp-2021-948
Preprint. Discussion started: 21 December 2021

Atmospheric Chemistry and Physics Discussions

all detected data (i.e. VOCs, trace gases and meteorological parameters) into the model with all reaction pathways of the MCM mechanism, and the SC2 disabled the PAN chemistry, which is the only difference between SC1 and SC2.

PAN could affect O_3 production by acting as a temporary source of NOx or sink of PA radical to affect precursors and radical chemistry in the troposphere (Xia et al., 2021). To quantify the changes of O_3 in response to PAN chemistry in the coastal city, two parallel scenarios (SC1 and SC2) were conducted based on the OBM model. The SC1 was the base scenario putting all detected data (i.e. VOCs, trace gases and meteorological parameters) into the model with all reaction pathways (as the description in Section 2.2), and the SC2 disabled the PAN chemistry, which is the only difference between SC2 and SC1. Figure 7 shows the differences of O_3 net production rates $\triangle P(O_3)$, $\triangle OH$, $\triangle HO_2$, $\triangle RO_2$, $\triangle NO$ and $\triangle NO_2$ between the SC1 and the SC2. Negative and positive values represented the inhibition and promotion effects of PAN photochemistry on O_3 formation, respectively. Overall, PAN mostly inhibited the O_3 formation during the observation days. $\triangle P(O_3)$ had significantly positive correlations with $\triangle OH$ (R^2=0.96 in spring and 0.95 in autumn), $\triangle HO_2$ (R^2=0.91 and 0.96), $\triangle RO_2$ (R^2=0.86 and 0.86) and $\triangle NO_2$ (R^2=0.72 and 0.85), and negative correlation with $\triangle NO$ (R^2=-0.63 and -0.65). As shown in Fig. S6, the promotion effects of PAN on O_3 mainly happened during the periods of 11:00-16:00 LT, and most of them concentrated on PAN pollution episodes. The percentage of negative $\triangle P(O_3)$ values were 83% and 69% in spring and autumn, defined as “inhibition effect stages”. While the positive $\triangle P(O_3)$ values accounted for 17% and 31% in spring and autumn, defined as “promotion effect stages”.

Figure 8 shows the variations of modeled $P(O_3)$, O_3 budgets and ROx on the inhibition and promotion effect stages in spring and autumn. The abundance of ROx in autumn (2.85×10^8 molecules cm^{-3}) was higher than that in spring (2.08×10^8 molecules cm^{-3}) during inhibition effect stages, while the $P(O_3)$ value in autumn (5.24 ppbv h^{-1}) was higher than that in spring (4.88 ppbv h^{-1}). On the contrary, the level of ROx in spring (4.81×10^8 molecules cm^{-3}) was higher than that in autumn (4.20×10^8 molecules cm^{-3}) during promotion effect stages, and the $P(O_3)$ value (5.95 ppbv h^{-1}) in spring was higher than that in autumn (5.76 ppbv h^{-1}). The results indicated that high ROx concentration was an important factor for the formation of O_3. In the case of closing PAN photochemistry, the $P(O_3)$ increased 1.20 and 1.12 times during inhibition effect stages and decreased 1.09 and 1.08 times during promotion effect stages in spring and autumn, respectively (Fig. 8a). This was consistent with the corresponding changes of ROx radical (Fig. 8b). During the inhibition effect stages, the averaged concentrations of OH, HO_2 and RO_2 increased 1.05, 1.16, and 1.17 times in spring, and increased 1.04, 1.10, and 1.12 times in autumn. During the promotion effect stages, the averaged concentrations of OH, HO_2 and RO_2 decreased 1.02, 1.03, and 1.06

https://doi.org/10.5194/acp-2021-948
Preprint. Discussion started: 21 December 2021

Atmospheric Chemistry and Physics Discussions

times in spring, and decreased 1.02, 1.04, and 1.05 times in autumn. These results indicated that the changes in ROx dominated the $P(O_3)$ trend without PAN photochemistry. Furthermore, the $P(O_3)$ level during promotion effect stages (5.95 ppbv h^{-1} in spring, 5.76 ppbv h^{-1} in autumn) was higher than that during inhibition effect stages s (4.88 ppbv h^{-1} in spring, 5.24 ppbv h^{-1} in autumn). For model-simulated $P(O_3)$ and O_3 budgets (Fig. 8a), HO_2+NO (account for 70±4%) and RO_2+NO (30±6%) were the main pathways of O_3 formation, and the main loss reactions were OH+NO_2 (83±12%).

PAN competed with O_3 precursors and terminated the radical chain to suppress O_3 formation by decreasing the ROx production during the inhibition effect stages. During the promotion effect stages, the intensive atmospheric oxidation capacity and photochemical reaction enhance the ROx formation rates from PAN to promote O_3 formation (Fig. 8b).

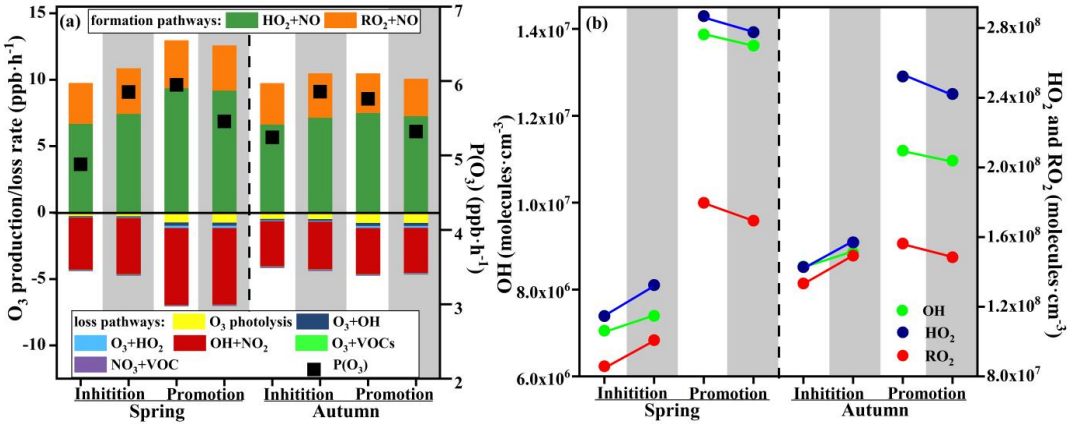

Fig. 8. Model-simulated (a) net O_3 production rate and O_3 budgets, (b) OH, HO_2 and RO_2 on the inhibition effect stages and promotion effect stages. Note: the white background parts represent the SC1 scenarios using the MCM mechanism, and the gray background parts represent the SC2 scenarios using the MCM mechanism with PAN chemistry disabled.

Table S4 showed the air pollutants and meteorological parameters during the inhibition effect stages and promotion effect stages. In detail, the mixing ratios of CO and the precursors of O_3 and PAN during the inhibition effect stages were significantly higher than those during the promotion effect stages. However, the $PM_{2.5}$ level during the inhibition effect stages was relatively lower than that during the promotion effect stages, reflecting the influence of heterogeneous reactions on $PM_{2.5}$ by suppling key photochemical oxidants to enhance PAN production (Xu et al., 2021). In addition, SO_2 and wind speed were comparable during the two scenarios. During the promotion effect stages, UV and T were significantly high, while P and RH were significantly low ($P<0.01$). Meanwhile, the PAN (1.89 in spring, 1.58 ppbv in autumn) and O_3 (50.26 ppbv in spring and 53.51 in autumn) under the promotion effects

https://doi.org/10.5194/acp-2021-948
Preprint. Discussion started: 21 December 2021

Atmospheric Chemistry and Physics Discussions

were higher than those under the inhibition effects (PAN: 1.04 and 0.84 ppbv; O_3: 27.32 and 36.42 ppbv in spring and autumn, respectively).

In general, ROx radicals dominated the atmospheric oxidative capacity and were the indicators of atmospheric photochemical reaction (Li et al., 2018). According to Section 3.2 of GAM analysis, we chose the factors of NO, TVOCs, $PM_{2.5}$, UV, T, RH, WS, and △ROx (△ROx=△OH+△HO_2+△RO_2), to discuss the key influencing factor under promotion effect stages. Here, the △P(O_3) rate and the relevant influencing factors were set as the response and explanatory variables, respectively. Table 2 showed the influencing factors on △P(O_3) under promotion effects in spring and autumn. The factors that did not pass the significance test were deleted. As the adjusted model showed, the adjusted R^2 and deviance explained for the smoothed variables in four GAM models ranged from 0.67~0.78 and 70%~80%, verifying the good fitting effect of the multiple-factor GAM model. According to the F-values, the effects of △ROx (21.56 in spring; 45.45 in autumn) and UV (9.66 in spring; 30.55 in autumn) were the main factors leading to the promotion effect in both seasons. Both △ROx and UV had significant positive non-linear relationships with △P(O_3) during promotion effect stages in both seasons (Fig. S7 and S8). The minor influences of WS and T were observed in autumn. The promotion effects easily happened during periods of favorable meteorological conditions for photochemical reactions.

Liu et al. (2021) found that PAN photochemistry inhibited O_3 production under low-NOx and low-ROx conditions, and promoted O_3 formation under high-NOx. However, in this study, sufficient NOx would not be the limited factor and the change of NOx could be ignored. Whether PAN photochemistry suppressed or enhanced O_3 production mainly depended on the meteorological conditions of photochemical reaction and the ROx levels.

Table 2 Estimated degree (during promotion effect scenarios in spring and autumn) of freedom (Edf), degree of reference (Ref. df), P-value, F-value, deviance explained (%), adjusted R^2, deviance contribution (%) for the smoothed variables (including NO, △ROx, TVOCs, $PM_{2.5}$, UV, T, RH, and WS) in the multiple-factor GAM model.

	Incipient				Adjusted			
Smoothed variables	Edf	Ref.df	F-value	P-value	Edf	Ref.df	F-value	P-value
Promotion effect stages in spring								
NO (ppbv)	5.58	6.39	2.09	0.06			Delete	
ROx (molecules·cm^{-3})	5.99	7.06	22.88	0.00	5.72	6.83	21.56	0.00
TVOCs (ppbv)	1.14	1.26	0.60	0.40			Delete	
$PM_{2.5}$ (ppbv)	1.98	2.51	2.62	0.07			Delete	
UV (W·m^{-2})	3.89	4.80	7.40	0.00	2.98	3.73	9.66	0.00
T (℃)	1.00	1.00	1.88	0.17			Delete	
RH (%)	1.00	1.00	0.86	0.36			Delete	
WS (m·s^{-1})	1.41	1.71	3.03	0.13			Delete	

https://doi.org/10.5194/acp-2021-948
Preprint. Discussion started: 21 December 2021

Atmospheric Chemistry and Physics Discussions

Promotion effect stages in autumn								
NO (ppbv)	1.15	1.28	0.20	0.66			Delete	
ROx (molecules·cm^{-3})	7.10	8.06	41.04	0.00	7.37	8.26	45.45	0.00
TVOCs (ppbv)	1.00	1.00	0.00	0.97			Delete	
$PM_{2.5}$ (ppbv)	1.00	1.00	0.53	0.47			Delete	
UV (W·m^{-2})	3.11	3.87	28.90	0.00	3.07	3.83	30.55	0.00
T (°C)	2.26	2.87	4.73	0.01	2.28	2.88	7.41	0.00
RH (%)	1.50	1.87	0.58	0.62			Delete	
WS (m·s^{-1})	4.67	5.76	2.73	0.02	4.53	5.60	3.66	0.00

4. Conclusions

Field observation was continuously conducted in spring and autumn in a coastal city of Southeast China. We clarified the seasonal variations of PAN pollution, formation mechanisms, influencing factors and impacts on O_3 production. The average levels of PAN in autumn were lower than that in spring, while the O_3 showed the opposite characteristics. The multiple-factor GAM model showed that the key factors on PAN mixing ratio were UV, Ox, and T in spring, while Ox, TVOCs, T and $PM_{2.5}$ played important roles in PAN formation in autumn. The MCM model is an ideal tool to explore PAN photochemical formation and its key precursors at the species level and provides more relevant suggestions for reducing photochemical pollution. The controlling emissions of aromatics and alkenes with ≤5 carbons were benefit for PAN pollution mitigation, and carbonyl compounds especially acetaldehyde were dominant in the PAN production mechanism. PAN presented the inhibition or promotion effects on O_3 under different environmental conditions. The promotion effects of PAN on O_3 mainly happened during the periods of 11:00-16:00 LT, most of which concentrated on PAN pollution episodes. According to the GAM analysis, the levels of ROx and UV were the main factors leading to the promotion effects in both seasons. Overall, PAN stimulated O_3 formation under high levels of UV, T and ROx in the coastal city. These results indicate that the monitoring of PAN and its precursors and the quantification of its impacts on O_3 formation have significant guidance on photochemical pollution control. The scientific analysis methods used in this study provide a reference for the research on the formation mechanism of PAN and O_3 in other regions.

Authorship Contribution Statement

Taotao Liu performed chemical modeling analyses of OBM-MCM and wrote the paper. Taotao Liu collected the data, contributed to the data analysis. Jinsheng Chen and Youwei Hong designed and revised the manuscript. Jinsheng Chen supported funding of observation and research. Gaojie Chen, Lingling Xu, Mengren Li, Yanting Chen, Xiaoting Ji, Chen Yang, and Yuping Chen contributed to discussions of results. Weiguo Huang, Quanjia Huang and Hong Wang provided part of the data in Xiamen.

https://doi.org/10.5194/acp-2021-948
Preprint. Discussion started: 21 December 2021

Atmospheric Chemistry and Physics Discussions

Acknowledgment:

This study was funded by the Cultivating Project of Strategic Priority Research Program of the Chinese Academy of Sciences (XDPB1903), the FJIRSM&IUE Joint Research Fund (RHZX-2019-006), the Center for Excellence in Regional Atmospheric Environment, CAS (E0L1B20201), the Xiamen Youth Innovation Fund Project (3502Z20206094), the foreign cooperation project of Fujian Province (2020I0038) and Xiamen Atmospheric Environment Observation and Research Station of Fujian Province.

Reference:

Atkinson, R., Baulch, D.L., Cox, R.A., Crowley, J.N., Hampson, R.F., Hynes, R.G., et al.: Evaluated kinetic and photochemical data for atmospheric chemistry: volume II gas phase reactions of organic species. Atmos. Chem. Phys. 6, 3625–4055, 2006.

Cardelino, C. A., Chameides, W. L.: An observation-based model for analyzing ozone precursor relationships in the urban atmosphere. J. Air Waste Manag. Assoc. 45, 161-180, 1995.

Chen, T., Xue, L., Zheng, P., Zhang, Y., Liu, Y., Sun, J., Han, G., Li, H., Zhang, X., Li, Y., Li, H., Dong, C., Xu, F., Zhang, Q., and Wang, W.: Volatile organic compounds and ozone air pollution in an oil production region in northern China, Atmospheric Chemistry and Physics, 20, 7069-7086, 10.5194/acp-20-7069-2020, 2020.

Elshorbany Y. F., Kurtenbach R., Wiesen P., et al.: Oxidation capacity of the city air of Santiago, Chile, Atmos. Chem. Phys., 8 (6), 2257-2273, 2008.

Fischer, E. V., Jacob, D. J., Yantosca, R. M., Sulprizio, M. P., Millet, D. B., Mao, J., et al.: Atmospheric peroxyacetyl nitrate (PAN): a global budget and source attribution. Atmos. Chem. Phys. 14, 2679–2698, 2014.

Fischer, E. V., Jaffe, D. A., Reidmiller, D. R., Jaegle, L.: Meteorological controls on observed peroxyacetyl nitrate at Mount Bachelor during the spring of 2008. J. Geophys. Res. Atmos. 115, 18, 2010.

Gaffney J S, Marley N, Cunningham M M, et al.: Measurements of peroxyacyl nitrates (PANS) in Mexico city: implications for megacity air quality impacts on regional scales. Atmos. Environ., 33 (30), 5003-5012, 1999.

Grosjean, E.; Grosjean, D.; Woodhouse, L. F.; Yang, Y. J. Peroxyacetyl nitrate and peroxypropionyl nitrate in Porto Alegre, Brazil. Atmos. Environ., 36, 2405–2419, 2002.

Guan L, Liang Y, Tian Y, Yang Z, Sun Y, Feng Y: Quantitatively analyzing effects of meteorology and $PM_{2.5}$ sources on low visual distance. Sci. Total Environ., 659, 764-772, 2019.

Han, J., Lee, M., Shang, X., Lee, G., Emmons, L. K.: Decoupling peroxyacetyl nitrate from ozone in Chinese outflows observed at Gosan Climate Observatory. Atmos. Chem. Phys. 17 (17), 10619-10631,

https://doi.org/10.5194/acp-2021-948
Preprint. Discussion started: 21 December 2021

2017.

He X, Lin Z S: Interactive effects of the influencing factors on the changes of $PM_{2.5}$ concentration based on GAM model. Environmental Science, 38 (1), 22-32, 2017.

Hu, B., Liu, T., Hong, Y., Xu, L., Li, M., Wu, X., Wang, H., Chen, J., and Chen, J.: Characteristics of peroxyacetyl nitrate (PAN) in a coastal city of southeastern China: Photochemical mechanism and pollution process, Sci Total Environ, 719, 137493, 10.1016/j.scitotenv.2020.137493, 2020.

Hua J, Zhang Y, de Foy B, Shang J, Schauer J. J, Mei X, Sulaymon ID, Han T: Quantitative estimation of meteorological impacts and the COVID-19 lockdown reductions on NO_2 and $PM_{2.5}$ over the Beijing area using Generalized Additive Models (GAM). J Environ Manage, 291:112676, 2021.

Kleindienst T. E.: Recent developments in the chemistry and biology of peroxyacetyl nitrate. Research on Chemical Intermediates, 20 (3-5), 335-384, 1994.

Li, B., Ho, S. S. H., Gong, S., Ni, J., Li, H., Han, L., Yang, Y., Qi, Y., and Zhao, D.: Characterization of VOCs and their related atmospheric processes in a central Chinese city during severe ozone pollution periods, Atmos. Chem. Phys., 19, 617-638, 10.5194/acp-19-617-2019, 2019.

Li, L., Dai, D., Deng, S., Feng, J., Zhao, M., Wu, J., Liu, L., Yang, X., Wu, S., Qi, H., Yang, G., Zhang, X., Wang, Y., Zhang, Y.: Concentration, distribution and variation of polar organic aerosol tracers in Ya'an, a middle-sized city in western China. Atmos. Res. 120, 29-42, 2013.

Li, Z., Xue, L., Yang, X., Zha, Q., Tham, Y. J., Yan, C., Louie, P. K. K., Luk, C. W. Y., Wang, T., and Wang, W.: Oxidizing capacity of the rural atmosphere in Hong Kong, Southern China, Sci Total Environ, 612, 1114-1122, 10.1016/j.scitotenv.2017.08.310, 2018.

Liu, L., Wang, X., Chen, J., Xue, L., Wang, W., Wen, L., Li, D., and Chen, T.: Understanding unusually high levels of peroxyacetyl nitrate (PAN) in winter in Urban Jinan, China, J Environ Sci (China), 71, 249-260, 10.1016/j.jes.2018.05.015, 2018.

Liu, T., Hong, Y., Li, M., Xu, L., Chen, J., Bian, Y., Yang, C., Dan, Y., Zhang, Y., Xue, L., Zhao, M., Huang, Z., and Wang, H.: Atmospheric oxidation capacity and ozone pollution mechanism in a coastal city of Southeast China: Analysis of a typical photochemical episode by Observation-Based Model, Atmos. Chem. Phys. Discuss. [preprint], https://doi.org/10.5194/acp-2021-764, in review, 2021a.

Liu, T., Hu, B., Xu, X., Hong, Y., Zhang, Y., Wu, X., Xu, L., Li, M., Chen, Y., Chen, X., and Chen, J.: Characteristics of $PM_{2.5}$-bound secondary organic aerosol tracers in a coastal city in Southeastern China: Seasonal patterns and pollution identification, Atmospheric Environment, 237, 117710, 10.1016/j.atmosenv. 2020.117710, 2020a.

Liu, T., Hu, B., Yang, Y., Li, M., Hong, Y., Xu, X., Xu, L., Chen, N., Chen, Y., Xiao, H., and Chen, J.: Characteristics and source apportionment of $PM_{2.5}$ on an island in Southeast China: Impact of sea-salt and monsoon, Atmospheric Research, 235, 104786, 10.1016/j.atmosres.2019.104786, 2020b.

Liu, Y., Shen, H., Mu, J., Li, H., Chen, T., Yang, J., Jiang, Y., Zhu, Y., Meng, H., Dong, C., Wang, W., and

https://doi.org/10.5194/acp-2021-948
Preprint. Discussion started: 21 December 2021

Atmospheric Chemistry and Physics Discussions

571 Xue, L.: Formation of peroxyacetyl nitrate (PAN) and its impact on ozone production in the coastal
572 atmosphere of Qingdao, North China, Sci Total Environ, 778, 146265, 10.1016/j.scitotenv.2021.146265,
573 2021.

574 Lonneman, W.A., Bufalini, J.J., Seila, R.L.: PAN and oxidant measurement in ambient atmospheres.
575 Environ. Sci. Technol. 10 (4), 374-380, 1976.

576 Ma Y, Ma B, Jiao H, Zhang Y, Xin J, Yu Z: An analysis of the effects of weather and air pollution on
577 tropospheric ozone using a generalized additive model in Western China: Lanzhou, Gansu. Atmos.
578 Environ., 224:117342, 2020.

579 Marley, N. A.; Gaffney, J. S.; Ramos-Villegas, R.; Gonzalez, B. C.: Comparison of measurements of
580 peroxyacyl nitrates and primary carbonaceous aerosol concentrations in Mexico City determined in 1997
581 and 2003. Atmos. Chem. Phys., 7, 2277– 2285, 2007.

582 Monks P. S.: A review of the observations and origins of the spring ozone maximum. Atmos. Environ.,
583 34 (21), 3545-3561, 2000.

584 Moore D. P., Remedios J. J.: Seasonality of peroxyacetyl nitrate (PAN) in the upper troposphere and lower
585 stratosphere using the MIPAS-E instrument. Atmos. Chem. Phys., 10 (13), 6117-6128, 2009.

586 Penkett, S. A., Brice, K. A.: The spring maximum in Photooxidants in the northern hemisphere
587 troposphere. Nature 319, 655–657, 1986.

588 Roberts, J.M., Stroud, C.A., Jobson, B.T., Trainer, M., Hereid, D., Williams, E., Fehsenfeld, F., Brune,
589 W., Martinez, M., Harder, H.: Application of a sequential reaction model to PANs and aldehyde
590 measurements in two urban areas. Geophys. Res. Lett. 28, 4583-4586, 2001.

591 Rubio, M.A., Lissi, E., Villena, G., Caroca, V., Gramsch, E., Ruiz, A.: Estimation of hydroxyl and
592 hydroperoxyl radicals concentrations in the urban atmosphere of Santiago. J. Chil. Chem. Soc. 50 (2),
593 471–476, 2005.

594 Saunders, S. M., Jenkin, M. E., Derwent, R. G., and Pilling, M. J.: Protocol for the development of the
595 Master Chemical Mechanism, MCM v3 (Part A): tropospheric degradation of nonaromatic volatile
596 organic compounds, Atmos. Chem. Phys., 3, 161–180, doi:10.5194/acp-3-161-2003, 2003.

597 Slade, J.H., Knopf, D.A.: Multiphase OH oxidation kinetics of organic aerosol: The role of particle phase
598 state and relative humidity. Geophys. Res. Lett. 41, 5297-5306, 2014.

599 Sun, M., Cui, J.N., Zhao, X.M., Zhang, J.B.: Impacts of precursors on peroxyacetyl nitrate (PAN) and
600 relative formation of PAN to ozone in a southwestern megacity of China. Atmos. Environ. 231, 11, 2020.

601 Tan, Z., Lu, K., Jiang, M., Su, R., Wang, H., Lou, S., Fu, Q., Zhai, C., Tan, Q., Yue, D., Chen, D., Wang,
602 Z., Xie, S., Zeng, L., and Zhang, Y.: Daytime atmospheric oxidation capacity in four Chinese megacities
603 during the photochemically polluted season: a case study based on box model simulation, Atmos. Chem.
604 Phys., 19, 3493-3513, 10.5194/acp-19-3493-2019, 2019.

https://doi.org/10.5194/acp-2021-948
Preprint. Discussion started: 21 December 2021

Atmospheric Chemistry and Physics Discussions

605 Temple, P. J., Taylor, O. C.: World-wide ambient measurements of peroxyacetyl nitrate (PAN) and
606 implications for plant injury. Atmos. Environ. 17, 1583–1587, 1983.

607 Tyndall, G. S., Cox, R.A., Granier, C., Lesclaux, R., Moortgat, G. K., Pilling, M. J., et al.: Atmospheric
608 chemistry of small organic peroxy radicals. J. Geophys. Res. Atmos. 106, 12157–12182, 2001.

609 Wolfe, G.M., Cantrell, C., Kim, S., Mauldin, R.L., Karl, T., Harley, P., et al.: Missing peroxy radical
610 sources within a summertime ponderosa pine forest. Atmos. Chem. Phys. 14, 4715–4732, 2014.

611 Wu, X., Li, M., Chen, J., Wang, H., Xu, L., Hong, Y., Zhao, G., Hu, B., Zhang, Y., Dan, Y., and Yu, S.:
612 The characteristics of air pollution induced by the quasi-stationary front: Formation processes and
613 influencing factors, Sci Total Environ, 707, 136194, 10.1016/j.scitotenv.2019.136194, 2020.

614 Wu, X., Xu, L., Hong, Y., Chen, J., Qiu, Y., Hu, B., Hong, Z., Zhang, Y., Liu, T., Chen, Y., Bian, Y.,
615 Zhao, G., Chen, J., and Li, M.: The air pollution governed by subtropical high in a coastal city in Southeast
616 China: Formation processes and influencing mechanisms, Sci Total Environ, 692, 1135-1145,
617 10.1016/j.scitotenv.2019.07.341, 2019.

618 Xia S Y, Zhu B, Wang S X, et al.: Spatial distribution and source apportionment of peroxyacetyl nitrate
619 (PAN) in a coastal region in southern China. Atmos. Environ., 260 (C4):118553, 2021.

620 Xu, W., Zhang, G., Wang, Y., Tong, S., Zhang, W., Ma, Z., Lin, W., Kuang, Y., Yin, L., and Xu, X.: Aerosol
621 Promotes Peroxyacetyl Nitrate Formation During Winter in the North China Plain, Environ Sci Technol,
622 55, 3568-3581, 10.1021/acs.est.0c08157, 2021.

623 Xu, X., Zhang, H., Lin, W., Wang, Y., Xu, W., Jia, S.: First simultaneous measurements of peroxyacetyl
624 nitrate (PAN) and ozone at Nam Co in the central Tibetan Plateau: impacts from the PBL evolution and
625 transport processes. Atmos. Chem. Phys. 18, 5199–5217. https://doi.org/10.5194/acp-18-5199-2018,
626 2018.

627 Xue, L., Wang, T., Wang, X., Blake, D.R., Gao, J., Nie, W., et al.: On the use of an explicit chemical
628 mechanism to dissect peroxy acetyl nitrate formation. Environ. Pollut. 195, 39–47, 2014.

629 Xue, L., Gu, R., Wang, T., Wang, X., Saunders, S., Blake, D., Louie, P. K. K., Luk, C. W. Y., Simpson, I.,
630 Xu, Z., Wang, Z., Gao, Y., Lee, S., Mellouki, A., and Wang, W.: Oxidative capacity and radical chemistry
631 in the polluted atmosphere of Hong Kong and Pearl River Delta region: analysis of a severe
632 photochemical smog episode, Atmos. Chem. Phys., 16, 9891–9903, 10.5194/acp-16-9891-2016, 2016.

633 Yan, R. E., Ye, H., Lin, X., He, X., Chen, C., Shen, J.D., Xu, K.E., Zhen, X. Y., Wang, L. J.: Characteristics
634 and influence factors of ozone pollution in Hangzhou. Acta Sci. Circumstantiae, 38 (3), 1128–1136, 2018.

635 Yuan, J., Ling, Z., Wang, Z., Lu, X., Fan, S., He, Z., Guo, H., Wang, X., and Wang, N.: PAN–Precursor
636 Relationship and Process Analysis of PAN Variations in the Pearl River Delta Region, Atmosphere, 9,
637 372, 10.3390/atmos9100372, 2018.

638 Zeng, L. W., Fan, G. J., Lyu, X. P., Guo, H., Wang, J. L., Yao, D. W.: Atmospheric fate of peroxyacetyl
639 nitrate in suburban Hong Kong and its impact on local ozone pollution. Environ. Pollut. 252, 1910–1919,
640 2019.

https://doi.org/10.5194/acp-2021-948
Preprint. Discussion started: 21 December 2021

Atmospheric Chemistry and Physics Discussions

641 Zhang, B. Y., Zhao, X. M., Zhang, J. B.: Characteristics of peroxyacetyl nitrate pollution during a 2015
642 winter haze episode in Beijing. Environ. Pollut. 244, 379-387, 2019.

643 Zhang, G., Mu, Y. J., Zhou, L. X., Zhang, C. L., Zhang, Y. Y., Liu, J. F., Fang, S. X., Yao, B.: Summertime
644 distributions of peroxyacetyl nitrate (PAN) and peroxypropionyl nitrate (PPN) in Beijing: understanding
645 the sources and major sink of PAN. Atmos. Environ. 103, 289-296, 2015a.

646 Zhang, G., Mu, Y. J., Zhou, L. X., Zhang, C. L., Zhang, Y. Y., Liu, J. F., Fang, S. X., Yao, B.: Summertime
647 distributions of peroxyacetyl nitrate (PAN) and peroxypropionyl nitrate (PPN) in Beijing: understanding
648 the sources and major sink of PAN. Atmos. Environ. 103, 289-296, 2015.

649

650